

Highly accurate geometric correction of satellite images of mountain areas

DING Kun, LONG Xiaomin, WANG Yanxia, ZHOU Ruliang

Southwest Forestry University, Yunnan Kunming 650224, China

Abstract: Highly accurate geometric correction is fundamental to the application of satellite images. In highly accurate geometric correction of remote sensing images for precise match to the base maps, the difficulties in capturing ground control points (GCPs), insufficient number of GCPs and low accuracy of the geo-referenced images remain to be frequent issues. In search for solutions to these issues, this paper proposes a new method for the geometric correction of satellite images for the mountain areas based on the terrain feature lines extracted from the Digital Elevation Model (DEM). This method uses DEM as the base maps without any geometric distortion for the geometric correction of satellite images. This paper presents the theories and method to extract terrain feature lines, such as gorges, mountain ridges, peaks and concaves and describes the procedures for the geometric correction for satellite images of mountain areas based on the terrain feature lines. It further discusses the problems in extracting terrain feature lines and capturing of GCPs, as well as the solutions to these issues. The outcome from the experiments shows the number of terrain feature lines of mountains areas are a great many times of those in the conventional map layers of hydrological systems and road networks, and that terrain feature lines extracted from DEM present high stability and reliability and can be applied in the highly accurate geometric correction for satellite images of mountain areas. The results of statistical test show the average geometric error is reduced to the size of one pixel when this method is used in geometric correction.

Key words: terrain feature lines, satellite image, highly accurate geometric correction

CLC number: TP751.1 **Document code:** A

Citation format: Ding K, Long X M, Wang Y X and Zhou R L. 2010. Highly accurate geometric correction of satellite images of mountain areas. *Journal of Remote Sensing*. **14**(2): 272—282

1 INTRODUCTION

Highly accurate geometric correction of remote sensing satellite images is fundamental to the application of remote sensing technology. After geometric correction at the system level, random errors of up to the dimensions of several pixels remain in the satellite images, e.g. NOAA/AVHRR images corrected at system level still maintain the errors of 1-6 pixels which adversely affect its application in assessing agricultural yields and monitoring of forest fires (Lip, 1994; Emery, 1989; Huang *et al.*, 2000; Zhao & Jing, 2000; Wang, 1999). This type of errors is generally random and presents unevenness and irregularity in spatial distribution and is attributable to mainly the curvature and undulated topography on the Earth's surface, changes in the internal and external positions of the satellite sensors, atmospheric reflections, and random changes in satellite's attitude. Therefore, in actual application of satellite images, highly accurate geometric correction is often necessary (Jiang *et al.*, 2004; Chen & Qin, 2005), in which using the GCPs (ground

control points) for highly accurate geometric correction is the main method for illuminating such errors of random distortion. Difficulties in capturing GCPs, insufficient number of GCPs as well as low resolution of images to be corrected are the problems existing in processing the satellite images with low- and medium resolutions. Using ground-truthed objects provides practical solution to the problem in high-accuracy correction of high-resolution satellite images but means very high cost (Zhao *et al.*, 2007; Ren *et al.*, 2001; Deng & Zhu, 2006), whereas high-accuracy correction of satellite images based on existing digital surveying and mapping products is the most economical and practical method.

In the application of remotely-sensed data, geographic base maps are generally regarded as error and distortion free, and satellite images need to be precisely geo-referenced to the topographic base maps. The fact that base surveying and mapping products carry certain amount of errors may enlarge the random errors in the satellite images if they are to be precisely geo-referenced on the base maps. Using those ground objects that are distinctively identifiable on the satellite images, such as

Received: 2008-05-19; **Accepted:** 2009-06-01

Foundation: Key Research Fund Project of Yunnan Province (No. 2002C005Z), The Scientific and Technological Breakthrough Project of Yunnan Province (No. 2006SG26), and projects of Yunnan Provincial Education Department (No. 07C10429).

First author biography: DING Kun (1965—), female, Associate Professor. She graduated in the mathematics major from the Department of Mathematics, Yunnan University and engages in application of mathematics and applied research in GIS and remote sensing, and has published more than ten papers in relevant fields.

Correspondence author biography: ZHOU Ruliang, E-mail: Zhou_ruliang@163.com

hydrological systems, road networks and lakes, to control the geo-referencing of satellite images is a conventional approach for high-accuracy geometric correction, in which, the sufficient amounts of GCPs that are selected with high accuracy becomes the key to accomplish highly accurate correction. However, for satellite images with medium- and above resolution, distinctive ground objects such as roads and hydrological systems barely present. Difficulty in locating GCPs and insufficient number of GCPs turn out to be a major problem in real-world application. In high resolution satellite images, although fine road networks and hydrological systems can all be visualized, such point and line features may not be readily drawn on the geographic base maps and it is also difficult to implement geographic correction with existing digital vector maps. Digital Elevation Model (DEM) is the most stable data in geographic base maps that contain all the feature points and lines, or terrain feature lines. The method of using such terrain feature lines contained in the geographic base maps to correct the ransom geometric distortions and errors in satellite images is the most economical and operational solution to the problem. In highly accurate geometric correction, the selection of GCP files relies on naked-eye recognition and interactive operations. Searching and selection of GCPs using raster DEM or 3-dimension images generated from DEMs are susceptible to the subjective judgment and difficult manipulation that lead to low work-efficiency and substantial data errors. This paper proposes a method to use DEM to extract files of terrain feature lines, and based on which, to control and correct satellite images. Experiment data sets taken from DEM data and US LANDSAT ETM data at the scale of 1:50000 are processed in the research.

2 THEORY AND TECHNOLOGY

Satellite images of mountain areas present distinctly the stereo features of the landscape and contain abundant information about terrain feature lines, and the DEM data contain all the terrain feature points and lines at the equivalent scale, including ridges, gorges, peaks and concaves and so on. Selection of GCPs by using the feature structures of forking and turning points and applying common high-accuracy geometric correction methods, the high accuracy geometric correction of remote sensing satellite images can be accomplished which follows these major steps of extracting terrain feature lines, selection of GCP files, polynomial correction and processing, as well as error estimation.

2.1 Extraction of terrain feature lines

Topography of mountain areas is often complex and diverse where ridge and gorge lines reflect the undulations in terrain structure, and peaks and concaves represent the altitudinal structure of the topography. By applying raster analysis method, the simulation algorithm of flow direction, accumulation flow algorithm, algorithm for recognizing ground object elevation are programmed for extracting ridge lines, gorge lines, peaks

and concave points.

2.1.1 Extraction of Gorge Lines

Based on the watercourse simulation approach that describes the movement of surface substance from high to low elevations, the flow direction of each raster point is identified by using the method of largest slope of single flow direction. The accumulative water confluence on each raster point is computed based on the water-flow direction on each single raster point. A gorge, as is called, is a catchment area in topography. A threshold is set by human-machine interaction: when the accumulative water confluence at a given point is greater than the threshold, the point is taken as one the upper side of the gorge line. The thresholds are determined through human-machine interaction. The threshold is correlated to the DEM scale and the size of the raster point. Too high a value may lead to the loss of those terrain feature lines that describe small topography, whereas too low a value will form surfaces of closed lines for many lowlands, rather than the median line in the vicinity of the lowest gorge areas. Determination of adequate threshold is key step to the processing and analysis. Extraction of terrain feature lines based on the above theory includes the follows steps:

(1) Computing the flow direction of raster points. As illustrated in Fig. 1, 1, 2, 4, 8, 16, 32, 64 and 128 represent the eight flow directions of raster point A, e.g. due east, due southeast, due south, due southwest, due west, due northwest, due north and due northeast. Array-listing each raster point in the DEM, if the elevation in vicinities of a given raster point equals, the raster point has no flow direction and is recorded as zero. The single flow largest slope drop method bases on Eq. (1) to calculate slope drop of the eight flow directions of each raster point, in which the largest slope is to be taken as the flow direction of the given raster point.

$$\text{Drop} = \Delta z / \text{distance} \times 100 \quad (1)$$

Where, Drop is the value of slope drop between the neighboring raster points, Δz is the elevation difference between the adjoining raster points, and distance measures the length between the adjoining raster points. Array-listing each raster points give the direction of the slope drop in the DEM.

(2) Computing accumulative flow on raster point. The accumulative flow on raster point indicates the accumulative value of the number of grids that flow into a given raster point. The can only be one flow direction for each raster point. If the adjoining eight pixels of the given raster point is examined, the maximum inflow for the raster point can only be eight. In computing the accumulative flow of a raster point, all pixels

32	64	128
16	A	1
8	4	2

Fig. 1 Eight flow directions of raster point A

that flow into the given raster point are array-listed. In other word, the inflow points are searched along the inflow direction toward the high elevation until no more inflow points can be found. Then, counting all the pixel points of the given raster point generates its accumulative flow. On the basis of the above theory, an octree is used for modeling, in which, the root nodes of the entire octree are the raster points for which the accumulative flow will be calculated. The 1st level nodes has eight bifurcations which corresponds to the eight raster points of the given node, e.g. upper left, left, lower left, lower, lower right, right, upper right and upper (See Fig. 2 Inflow model of raster points). If a given flow direction of the eight child nodes points toward the parent node, then the bifurcation exists. Otherwise, the bifurcation is interrupted. Afterwards, child nodes for the 2nd level nodes can be built using the same method, until any child nodes at any level are not found. Counting all the nodes that derive from the root node on the octree will generate the accumulative flow; then remove the repeated computation with optimization algorithm.

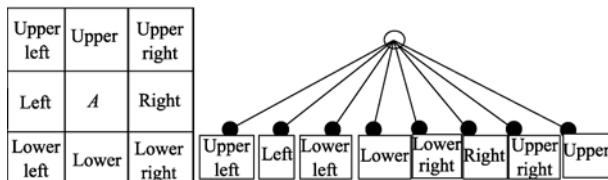


Fig. 2 Relation of the input of raster point *A* and parent node and child node in an octree

(3) Threshold identification. Plug in the raster data for accumulative flow and visualize in monochromatic map. High luminance marks areas with high accumulative flow. Rudimentary visual judgment of the gorge topography helps to select typical gorge areas for interactive queries to determine the threshold for the accumulative flow of a gorge. The first computation for extracting gorge features on the image is then conducted by array-listing all raster points: if the accumulative flow is greater than the threshold, then $M_{\text{gorge}}=1$, if not, $M_{\text{gorge}}=0$. M_{gorge} is the rasterized gorge map. Visualize M_{gorge} , and give a judgment on the extracted product. If the product is of poor visual effect, adjust the threshold until satisfactory visual effect is attained.

(4) Vectorization. Using common function to convert the rasterized catchment areas into vector lines, that is, the generation of gorge feature lines. Cleaning up of the vectorized maps is necessary to remove those very short and broken lines and speckles.

2.1.2 Extraction of ridge lines

Reversing the computation for the DEM, that is, to invert the high elevation areas into lowlands, and vice versa. Choosing appropriate M and apply the following conversion formula:

$$\text{DEM}_1 = M - \text{DEM}$$

Generally speaking, M should be two times of the original DEM elevation. After the topographical reversion of the original DEM, the new output is processed by repeating the methods in Section 2.1.1 to obtain the ridge line features.

2.1.3 Extraction of single peaks

In general, single peaks are point terrain features that are often higher in elevation than those neighboring objects. Smoothing is used to level the highlands on the original DEM. By comparing the newly processed DEM with the original ones, those points with significant leveling are peak points. Using general resampling method to resample the original DEM in which the pixel size should be two times of the original to generate the new DEM. The new DEM is then repeatedly processed two to three times by applying data smoothing with filtering kernels. By calculating the differences between the original and the latest DEMs with the methods given in (3) and (4) of Section 2.1.1, the vector data of peak points is obtained.

2.1.4 Extraction of point concave features

By using inversed computing of the DEM as described in Section 2.1.2, single point concaves can be obtained by repeating the method in Section 2.1.3.

2.2 Selection of GCPs

In the common map visualization and editing environment in a GIS interface, input the ETM satellite imagery corrected at the system level and display in false color; input gorge lines and display in blue; input ridge lines and display in red; input the map layer of mountain peaks and display in red, and also the concave layer visualized in red spots. The needed GCPs for gorges can be selected by manual manipulation using the matching method for homonymy ground objects (points) through collecting the coordinates of the feature points in the gorges or concaves, as well as the coordinates of the same objects/points from the corresponding satellite imageries. Rotate all the datasets by 180 degrees and collect the GCPs for mountain ridges and generate the GCP files.

2.3 Rectification processing

As errors from random distortion inherently maintain unevenness and inconsistency, the perimeters of each and every area on satellite images have their own GCPs which imply inadequacy in geometric correction with higher polynomial or rational function methods for the entire area; in this case, self-adaptive correction based on the triangle network is adopted.

2.4 Error estimation

The errors resulting from geometric correction of satellite imageries are random variables that obey normal distribution by error theories. Then, the errors can be estimated based on with statistical test, The sample points for error estimation are obtained by using the following operations: create a map layer of kilometer grid with a starting point that satisfies the randomness needs; Use the grid points as the measurement unit to take random samples; look for the distinctly identifiable ground objects located closest to a given grid point; Use the map layer of terrain feature lines to measure the geometric errors that exist

in the satellite imagery on the computer screen. The aggregate of errors on each grid point X_1, X_2, \dots, X_n form the samples of joint accumulative distribution for error estimation, in which the mean value ΔX is taken to estimate the total error using the following formula for ΔX :

$$\Delta X = \frac{(X_1 + X_2 + \dots + X_n)}{n} \quad (2)$$

where, n is the number of samples and the confidence interval for confidence $1-\alpha$ is:

$$(\Delta X - St_{\alpha/2}(n-1)/n^{1/2}, \Delta X + St_{\alpha/2}(n-1)/n^{1/2}) \quad (3)$$

Where, $S^2 = \{(X_1 - \Delta X)^2 + (X_2 - \Delta X)^2 + \dots + (X_n - \Delta X)^2\} / (n-1)$. $t_{\alpha/2}(n-1)$ is the two-way quantile for $t(n-1)$ distribution.

3 EXPERIMENT RESULTS

3.1 Target area for the experiment

The target area for this data processing experiment is Anning City that adjoins Kunming City and located between $E102^\circ10' - 102^\circ37'$ and $N24^\circ31' - 25^\circ06'$. Anning is located on the eastern brim of the Central Yunnan Plateau where the landscape is conspicuously undulating and belongs to mid-mountain physiognomy.

3.2 Data preparation

The Enhanced Thematic Mapper (ETM) satellite image that Southwest Forestry University procured from Chinese Academy of Sciences in 2000 is used for the experiment. Specifications of the satellite image are as follows: Satellite orbit parameters WRS (World Reference System): 129/043; array size: 6969 columns by 5965 lines; sun altitude: 52.4 and sun azimuth: 139.8; scene center at $E103^\circ5'0'' - N24^\circ33'0''$. It is a product generated from system-level geometric correction and a near-true color composite satellite image by compositing RGB band 5, 4 and 3.

A map layer of contours generated from a relief map with a scale of 1 : 50000 is used as base data for extracting the terrain feature lines.

3.3 Extraction and results of terrain feature lines

3.3.1 DEM generation and processing

The digitized contours (scale: 1 : 50000) is input for generating TIN data, which is then converted into raster data arrays with a resolution of 10 m, or the DEM, which is smoothed, noises eliminated and false depression points cleared.

3.3.2 Extraction of and results from terrain feature lines

In the ArcGIS Workstaion environment, a computer program tool is written in AML programming language for automated extraction and processing of gorge and ridge lines. Through multiple experiments and adjustment of thresholds, satisfactory results are obtained when L is assigned the value of 60. Fig. 3 presents the effect of a product from overlaying the gorge and ridge lines extracted from DEM on the 3-dimension image in

which blue vector lines are the gorge lines, and red vector lines the ridge lines.

Fig. 4 gives a visual display of overlaying gorge lines extracted from the DEM and hydrology system from the relief map (scale: 1:50000) on the satellite imagery. It is obvious that the vector data for the hydrology system and gorge lines are not of the same scale of data quantity: hydrological lines present only in large watersheds whereas gorge lines show up in any undulating topography. Therefore, it is quite feasible to control the correction of random geometric distortions on the satellite image wherever there is undulating topography.

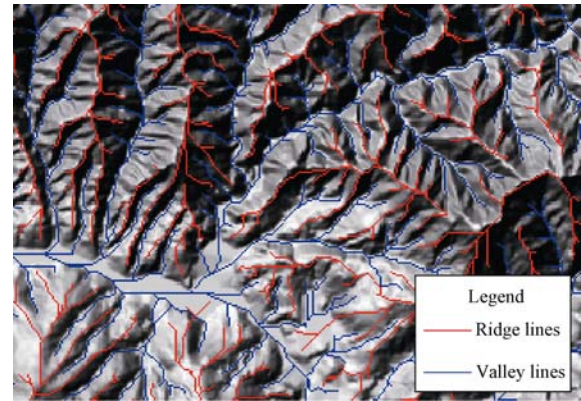


Fig. 3 A Visual presentation of overlaying extracted ridge (red) and gorge lines (blue) on a topographic map

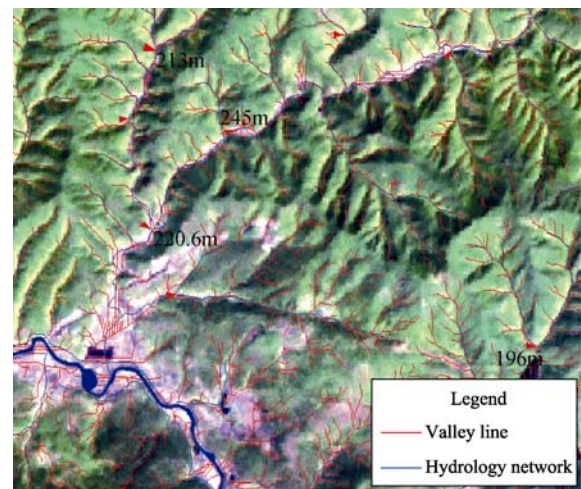


Fig. 4 Overlay visualization of gorge and river lines on a satellite image

3.4 Extraction and correction of Ground Control Points (GCPs)

A GCP collection program is written in AML to perform the operations of adding, deleting, saving GCPs and exit from the program to allow the interactive selection of GCPs in large batches. In the area of more than 1000 km² of Anning City, the GCPs created in the FGCP file reach as high as 1175. During the GCP selection, those crosses and turning points with good visual effect on the satellite images are chosen as the GCPs.

Moreover, GCPs should also be located to small locals on the satellite image. The territory of Anning City is very fragmented and undulating, therefore, dense GCP collection can be attained by using gorge lines; therefore, the GCPs in the experiments are mainly taken from the gorge lines.

3.5 High accuracy correction and error estimation based on the terrain feature lines

Geometric correction is processed in a Workstation environment and image with nearly perfect rectification is obtained. Those identifiable topographical features represented in the satellite image are accurately rectified with most of the gorge lines.

From graticules created with 0.02° intervals and codes assigned to the grids, a small sample of 20 grid points is randomly selected, as shown in Fig. 5. Base on projection of the graticule map and taking the gorge lines as true value, the errors of the grid points selected as samples are measured by using an integrative method to obtain the sample data (See Table 1).

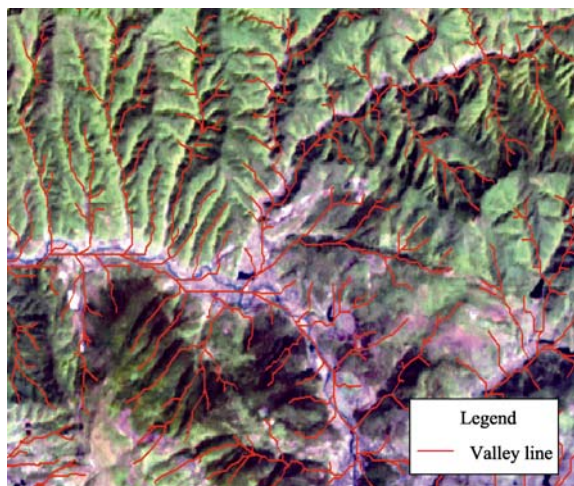


Fig. 5 Interaction interface of GCP collection

Table 1 Sample points used in error estimation

Code	Error/m
01	28.63
02	16.98
03	30.35
04	41.55
05	26.88
06	34.28
07	56.35
08	29.86
09	22.32
10	46.53
11	34.63
12	12.87
13	22.23
14	9.11
15	35.30
16	24.16
17	34.71
18	24.68
19	42.40
20	35.24

Applying Eq. (2) gives an overall average error of: $\Delta X=30.453$ $s=1.381$.

Taking the confidence of 90% and checking the two-way quantile table of T distribution with a 19 degree of freedom, the overall estimated interval is calculated to be (29.92, 30.99). With Eq. (3), the overall estimated interval is (29.92, 30.99).

The outcome from the experiment shows that the average geometric error is less than one pixel, or 30 m, and 90% of certainty leads to the judgment that the corrected error is between 29.92m and 30.99m.

4 CONCLUSIONS AND DISCUSSIONS

4.1 Conclusions

The following conclusions are drawn from the above study:

(1) The study proposes a set of theory and methodology for rectifying remote sensing satellite images of mountain areas by controlling terrain feature lines. This methodology is based on the special features of the DEM terrain feature lines to represent the topographical undulation and uses these features as baseline to implement highly accurate correction of the random geometric distortions of remote sensing satellite images.

(2) By replacing conventional control and correction of map layers with the new method based on the DEM terrain feature lines, the quantitative scale of control lines is greatly expanded, which provides solutions to the difficulties in identifying GCPs and insufficient number of GCPs.

(3) This method is applicable in the highly accurate geometric correction of satellite images for mountain areas with significant topographical undulation.

(4) Outcome from the experiment shows that the geometric error of satellite images after highly accurate correction is less than one pixel.

4.2 Discussions

Due to poor visibility of small roads and hydrological systems on remote sensing satellite images with a resolution below 10 m, there exist difficulties in locating GCPs and insufficient number of GCPs during the highly accurate geometric correction. In particular, in mountainous areas, due to the impact of projection distortion, there are only a few identifiable GCPs which lead to poor quality in some local areas in a corrected image. In areas of undulating topography gorge lines and ridge lines are often present, which can be extracted to create terrain feature lines with DEM data and used to control and correct the satellite images, as solutions to the aforementioned problems.

In the process of extracting the terrain feature lines, there are considerable difficulties in setting the threshold. In the case of too small a threshold, those small topographical features can not be sufficiently extracted, whereas those larger topographical features can not be presented in terrain feature lines if too large a threshold is set. In future practice, consideration should be given to acquire terrain features lines at various scales through manipulating multi-resolution and multi-temporal data sets.

In areas with insignificant topographic undulations, artificially enlarging elevation ratios can produce considerable topographic undulations for flat areas. The approach to apply this method to extract the terrain feature lines in areas with more flat landscape is worth further research attention.

In reversed DEM conversion, the M value can be taken to be 1.5—2 times of the highest elevation and will not affect the outcome of the analysis, as in nature it is a simple linear transformation. In the future, considerations should be given to topographic inversion by using inversely proportional inversion.

In the process of GCPs collection, due to visual limitations, it is generally easy to identify the correlations between a pseudo stereoscopic images and terrain feature lines of gorges, but difficult to identify such correlations between the terrain feature lines of mountain ridges. Certainly, due to erosion on the Earth's surface in the long past, relatively flattened ridges of some mountain peaks is another cause of such difficulties. Inverting all the spatial data by 180 degrees can be one practical method to collect the GCPs of mountain ridges, but it has not been further researched into in this study.

In the error estimation as discussed in the paper, mid-point estimation and interval estimation in statistics is used to estimate the errors in highly accuracy correction. The error generated from the mid-point error estimation is 33.25m which is the size of one pixel on the image and approximate to the error estimate in the study. As the performance of the highly-accurate correction effect in this study is assessed by the distance between the ground objects and the terrain feature lines, regardless of the plus-minus values, therefore, using the error estimate method in the paper help to ascertain the accuracy in the image correction.

As the multiband ETM image comes with a resolution of 30 m, when the image is enlarged to a scale of 1:20000, mosaic effect adversely affect not only GCP identification and selection by naked eyes but also the measuring and assessment of errors.

Data fusion of multiband images, sub-pixel decomposition and image enhancement contribute significantly to improving the visual effects and visible scales of satellite images.

REFERENCES

- Chen Y L and Qin J. 2005. Geometric correction for pretreatment of landsat-7 satellite image. *Railway Investigation and Surveying*, (4): 16—18
- Deng X J and Zhu J J. 2006. The geometric rectification of QuickBird images. *Modern Surveying and Mapping*, **28**(6): 40—41
- Emery W J. 1989. AVHRR image navigation: summary & review. *Photogrammetric Engineering and Remote Sensing*, **55**(8): 1175—1183
- Huang J F, Xu H W and Wang R C. 2000. Accurate geometric correction for NOAA/AVHRR data. *Journal of Zhejiang University (Agric. & Life Sci.)*, **26**(1): 17—21
- Jiang G M, Liu R G and Niu Z. 2004. An optimal geometric correction method for MODIS 1B data collection and its software development. *Journal of Remote Sensing*, **8**(2): 158—163
- Lip Donald. 1994. A one-step algorithm for correction and calibration of AVHRR level 1B data. *Photogrammetric Engineering & Remote Sensing*, **60**(2): 165—171
- Ren L C, Zhu C G and Zheng K. 2001. SOMP geometric exact correction method of TM image. *Journal of Remote Sensing*, **5**(4): 295—299
- Wang W Y. 1999. A study of forest fire monitoring by satellite and the relative problem of information transmission. *Forest Fire Prevention*, (4): 35—36
- Zhao B Y and Jing X F. 2000. Study of geometric correction technology and methods for TM data. *Soil and Water Conservation in China*, (6): 30—32
- Zhao J A, He R Y and Zhang S G. 2007. Geometric precision correction of the ETM+ Pan imagery. *Computer Simulation*, **24**(6): 199—202

地性线的山地区域的卫星影像几何精纠正

丁 琨, 龙晓敏, 王艳霞, 周汝良

西南林学院 云南省森林灾害预警与控制重点实验室, 云南 昆明 650224

摘要: 提出了一种山地区域基于DEM地性线的控制纠正新方法, 该方法以数字地形模型DEM为无几何变形的控制基准纠正卫星影像。阐述了提取沟谷、山脊、山峰和凹地区域的地性线的原理和算法, 给出了山地区域基于地性线进行卫星图像几何精纠正实施步骤, 进一步讨论了地性线提取、控制点采集存在的问题, 以及解决问题的途径。实验结果表明, 对于山地区域, 地性线的空间数量数倍于水系、道路等常规地图层; 地性线来源于DEM, 其空间稳定性和可靠性更高, 可以用于山地区域的卫星影像的严格控制纠正。用该方法进行几何纠正处理, 几何误差能控制在一个像元的水平上。

关键词: 地性线, 卫星影像, 几何精纠正

中图分类号: TP751.1 **文献标识码:** A

引用格式: 丁 琨, 龙晓敏, 王艳霞, 周汝良. 2010. 地性线的山地区域的卫星影像几何精纠正. 遥感学报, 14(2): 272—282
Ding K, Long X M, Wang Y X and Zhou R L. 2010. Highly accurate geometric correction of satellite images of mountain areas. *Journal of Remote Sensing*, 14(2): 272—282

1 引言

卫星遥感图像的几何精纠正遥感应用的基础, 经过系统级纠正后, 卫星遥感图像往往还存在若干个像元的随机误差, 如系统级纠正的 NOAA/AVHRR 图像还存在 1—6 个像元的误差, 影响了农业估产、森林火灾监测的应用(Lip, 1994; Emery, 1989; 黄敬峰等, 2000; 赵帮元 & 荆小峰, 2000; 王文元, 1999), 这种误差主要表现为随机误差, 在空间上的分布具有不均匀性、不规则性。这种随机误差主要来自于地球表面的曲率、地形起伏、传感器内外方位元素的变化、大气的折射、卫星姿态随机变化等的影响, 遥感数据应用时还要进行几何精纠正(蒋耿明等, 2004; 陈于林 & 秦军, 2005), 利用地面控制点(简称 GCP, Ground Control Points 的缩写)进行几何精纠正消除这种随机变形误差的主要方法。控制点难找、控制点不足、纠正图像精度不高是中低分辨率卫星影像处理时面对的难题, 用实测的 GPS 地物点是解决高分辨率卫星影像精纠正问题的一种方法, 但经济成本太高(赵君爱等, 2007; 任留成等, 2001; 邓晓嘉 & 朱建军, 2006), 基于现有的

数字化测绘成果实现遥感影像的精纠正是最经济、最实用的方法。

卫星遥感数据应用时, 一般认为基础地理底图是无误差、无变形的数据, 需要将卫星图像精确纠正到基础地理底图上。实际上, 基础测绘成果上也存在的一定误差, 要将卫星遥感影像严格匹配到基础地理底图上, 也会使遥感影像的随机误差加大。利用基础地理底图上的河流网、道路网、湖泊等卫星图像上可以识别的明显地物点来控制纠正卫星遥感影像, 是几何精纠正的传统方法。能选取足够多的、精度高的控制点, 是完成精纠正的关键。但对于中分辨率以上的卫星影像, 难以表现道路、水系等明显地物, 控制点难找、控制点不足是实际应用中的一大难题; 对于高分辨率卫星影像, 虽然非常细微的路网、水系网等能实现可视化, 但基础地理底图上可能没有这些特征点线, 也难以用现成的数字矢量图进行控制纠正。DEM(Digital Elevation Model, 数字地形模型)是地理底图最稳定的数据, 它包含该比例尺上的地形变化的所有特征点线, 即地性线, 利用 DEM 包含的地性线纠正卫星图像的随机几何变形和误差, 是解决问题的最经济和实用

收稿日期: 2008-05-19; 修订日期: 2009-06-01

基金项目: 云南省重点基金项目(编号: 2002C005Z), 云南省科技攻关项目(编号: 2006SG26)和云南省教育厅项目(编号: 07C10429)。

第一作者简介: 丁琨(1965—), 女, 副教授, 1986年毕业于云南大学数学系数学专业, 主要从事数学应用及遥感应用研究工作。

通讯作者: 周汝良, E-mail: Zhou_ruliang@163.com.

的好方法。几何精纠正处理中控制点文件的采集依赖于肉眼识别与交互操作, 直接用栅格格式的 DEM 或 DEM 生成的立体图像寻找和采集控制点, 受人的主观判断、操作不易等方面的影响, 工作效率低、数据误差大。文中提出了一种用 DEM 提取为矢量格式的地性线文件, 用基于 DEM 的地性线来控制纠正卫星影像的方法。并以 1:50000 比例尺 DEM 数据、美国陆地卫星 ETM 数据为实验数据, 进行了处理实验。

2 原理与方法

山地区域的卫星影像可以明显的反应地形的立体特征、包含丰富的地性线信息; DEM 数据中包含有该比例尺水平上的所有地物特征点线, 如山脊、沟谷、山峰、凹地等; 用地性线的分叉、转折点等特征结构点采集控制点, 再利用一般的几何精纠正方法, 即可完成卫星遥感影像的几何精纠正。

2.1 地性线的提取

山地地形复杂多样, 山脊线、沟谷线表达了地形的起伏结构, 山峰、凹地表达了地形的高低结构。利用栅格分析方法, 设计水流流向模拟算法、流量累积算法、地物的高点识别算法, 实现山脊线、沟谷线、山峰点、凹地点的提取。

2.1.1 沟谷线的提取

基于地表物质向低处运动的水流模拟方法, 利用单流向最大坡降法确定每个栅格点的流向; 依据每个栅格点上的水流方向, 可计算出每个栅格点的累计汇水量。所谓沟谷, 就是地形上的汇水区域, 确定阈值, 当某点上的汇水量大于该阈值时, 认为该点是沟谷线上的点。阈值依靠人机交互选取, 这个阈值与 DEM 的比例尺及其栅格点大小有关, 取值太大, 可能会导致表达小地形的地性线的丢失, 取值太小, 很多低地会形成面状闭合线, 而不是最低沟谷区域附近的中线, 合适的阈值是处理与分析的一个关键步骤。基于上述原理的地性线的提取包括了如下步骤:

(1) 栅格点的流向的计算。如图 1, 分别用 1, 2, 4, 8, 16, 32, 64, 128 代表栅格 A 流向正东、正东南、正南、正西南、正西、正西北、正北和正东北的 8 个方向, 遍历 DEM 的每个栅格点, 如果某个点周边的高程相等, 则该点无流向, 记为 0, 单流向最大坡降法就是依据式(1), 计算每个栅格点的 8 流向坡降值, 取最大坡降方向为该点的流向。

$$\text{Drop} = \Delta z / \text{distance} \times 100 \quad (1)$$

其中, Drop 为相邻栅格的坡降值, Δz 为相邻的栅格的高程差, distance 为相邻栅格的距离。

32	64	128
16	A	1
8	4	2

图 1 栅格点 A 的 8 流向

遍历每个栅格点可计算出 DEM 的坡降方向。

(2) 栅格点的累计流量的计算。栅格点的累计流量是指流入某个栅格点的栅格数的累计值。一个栅格点的流向只有一个方向, 但只考虑这个栅格点的周边 8 像元的时候, 流入这个栅格点的水流最多是 8, 计算一个栅格点的累计流量, 还要对整个地图中流入该点的像元遍历, 即沿流入方向, 向海拔高的地方寻找流入点, 直到无流入点时停止, 之后, 统计流入该点的所有像元点, 得到该点的累计流量。依据上面的原理, 使用 8 叉树建模, 整棵 8 叉树的根节点为需要计算累计流量的栅格点, 第 1 级子节点有 8 个分叉, 8 个分叉分别对应于该点的左上、左、左下、下、右下、右、右上、上共 8 个栅格点(图 2, 栅格点的流入模型), 如果这 8 个子节点的某个流向是向着父节点, 则该分叉存在, 否则, 该分叉截断; 之后, 对于第 2 级子节点, 如前面方法建立自己的儿子节点, 直到任何一级的任何子节点不存在儿子节点为止。之后, 统计根节点所生长的所有 8 叉树上的节点, 该数即为累计流量数。使用优化算法, 可去除重复计算量。

(3) 阈值的选取。调入累计流量栅格数据, 显示为单色地图, 亮度高为汇水量大的区域, 对沟谷地形做基本的目视判断, 选定沟谷的典型区进行交互查询, 确定沟谷的累计流量阈值。并对图像做第一次沟谷提取试算, 算法为: 遍历所有栅格点, 当累计流量大于阈值, $M_{\text{gorge}}=1$, 否则 $M_{\text{gorge}}=0$ 。 M_{gorge} 即为栅格化的沟谷地图。对 M_{gorge} 进行视

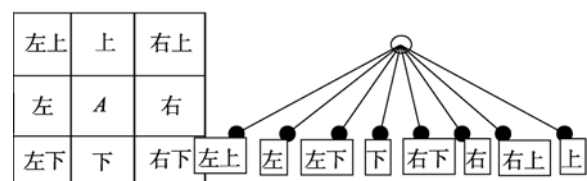


图 2 栅格点 A 的流入与 8 叉树的父节点与子节点的关系

化显示,判断提取效果,如果效果差,对阈值进行相应调整,直到满意为止。

(4)矢量化计算。使用一般的栅格到矢量的转换函数,将栅格化的流域区细化为线状的矢量线,即生成了沟谷特征线。之后,还要对矢量地图做适当的清洁处理,如去掉非常短小的断线等。

2.1.2 山脊线的提取

将 DEM 进行反转运算,把海拔高的区域变为低地,海拔低的区域变为高地。选择恰当的 M , 利用变换式:

$$DEM_1 = M - DEM$$

一般来说, M 最好取原 DEM 的最高高程的 2 倍。将原 DEM 实现地形反转之后,对新的 DEM_1, 重复 2.1.1 节的处理,即可得到山脊线。

2.1.3 单体山峰的提取

一般来说,单体山峰是点状地性线。山峰的海拔高于周边地物的海拔,将原 DEM 平滑处理,能起到削平高地的作用。将处理后的新的数字高程模型与原 DEM 比较,有较大削平作用的点即为山峰点。使用一般重采样方法,对原 DEM 重采样,像元尺寸取原来的 2 倍,得到新的数字地形模型,用平滑滤波方法对其进行 2—3 次平滑。把原 DEM 与新的数字高程模型做差值运算,用 2.1.1 节的(3)、(4)中的方法,计算出山峰点矢量数据。

2.1.4 点状凹地的提取

用 2.1.2 节做 DEM 的反转运算,用 2.1.3 节的方法提取单点凹地。

2.2 控制点的采集

在一般 GIS 系统的地图显示与编辑环境中,将经过系统级纠正的 ETM 卫星图像调入并显示为假彩色;调入沟谷线,用蓝色显示;调入山脊线,用红色表示;调入山峰地图,用红色的点显示;调入凹地地图,用红色点显示。手工交互采集纠正需要的沟谷控制点,即用同名地物点匹配方法,采集沟谷或凹地上的特征点以及其对应的卫星影像的同名地物点的坐标。将全部数据旋转 180° 后,采集山脊控制点,并生成控制点文件。

2.3 纠正处理

由于随机变形误差具有不均匀性、不一致性,卫星影像的每一小块区域周边有自己的控制点,不能使用适用于整体区域的高次多项式或有理函数纠正,使用的是自适应三角形网络法纠正。

2.4 误差估计

卫星图像几何纠正存在的误差是随机变量,依

据误差理论,其服从正态分布,依据统计理论估计误差。误差估计的样本点按如下方法实现,建立一个公里格网地图层,公里格网的起点满足随机性要求。以格网点为单元进行随机抽样。对于抽中的格网点,寻找离该格点最近的可辨别的明显地物点,以地性线图层为基准,在计算机屏幕上测量卫星图像存在的几何误差,各个格点上的误差集合 X_1, X_2, \dots, X_n 构成了误差估计的简单随机样本。用样本的均值 ΔX 估计总体误差。 ΔX 的估计式为:

$$\Delta X = \frac{(X_1 + X_2 + \dots + X_n)}{n} \quad (2)$$

这里, n 为样本容量。置信度为 $1-\alpha$ 的置信区间为:

$$(\Delta X - St_{\alpha/2}(n-1)/n^{1/2}, \Delta X + St_{\alpha/2}(n-1)/n^{1/2}) \quad (3)$$

这里, $S^2 = \{(X_1 - \Delta X)^2 + (X_2 - \Delta X)^2 + \dots + (X_n - \Delta X)^2\} / (n-1)$, $t_{\alpha/2}(n-1)$ 为 $t(n-1)$ 分布的 α 双侧分位数。

3 实验结果

3.1 实验区

数据处理实验区为毗连昆明的安宁市,位于东经 $102^\circ 10' - 102^\circ 37'$, 北纬 $24^\circ 31' - 25^\circ 06'$ 之间,地处滇中高原的东部边缘,境内地表起伏大,属中山地貌。

3.2 数据准备

使用西南林学院向中国科学院遥感卫星地面站购买的 2000 年的 ETM(Enhanced Thematic Mapper) 卫星遥感图像,卫星轨道号(WRS)是 129/043,阵列大小为 6969 列 \times 5965 行,太阳高度角 SUN ELEVATION = 52.4° , 太阳方位角 SUN AZIMUTH = 139.8° ,景中心位置为东经 $103^\circ 5' 0''$, 北纬 $24^\circ 33' 0''$,是系统级纠正处理后的数据产品。按 RGB543 的假彩色合成方法,合成近似真彩色的卫星图像。

采集的 1:50000 地形图上的等高线地图层,作为提取地性线处理的预备数据。

3.3 地性线的提取处理与结果

3.3.1 DEM 生成及处理

利用 1:50000 数字化等高线生成不规则三角网(TIN)数据;将 TIN 转化为 10m 分辨率的栅格阵列数据,即 DEM;对 DEM 进行平滑、去噪声等处理,去除伪下陷点。

3.3.2 地性线的提取处理与结果

在 ArcGIS 下 Workstaion 环境下,应用宏语言 AML 编写计算程序,进行沟谷线、山脊线的自动提取处理。通过多次试验和修改阈值,取 $L = 60$ 得到较好效果。见图 3, DEM 提取的沟谷线、山脊线与立

体地形影像的叠加效果, 蓝色矢量线为沟谷线、红色矢量线为山脊线。

DEM提取的沟谷线与1:50000地形图上河流及其卫星影像的叠加显示, 见图4, 可以明显看到, 水系线与沟谷线不是一个数量级别的矢量数据; 水系线仅仅在大流域区才出现, 沟谷线可以出现在任何地形起伏的地方。所以, 只要有地形起伏的地方, 都可以很好地控制纠正卫星图像上随机几何变形。

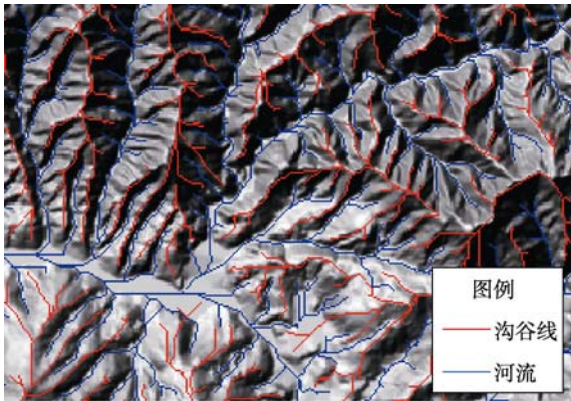


图3 提取的山脊线(红色)、沟谷线(蓝色)与地形图像的叠加显示

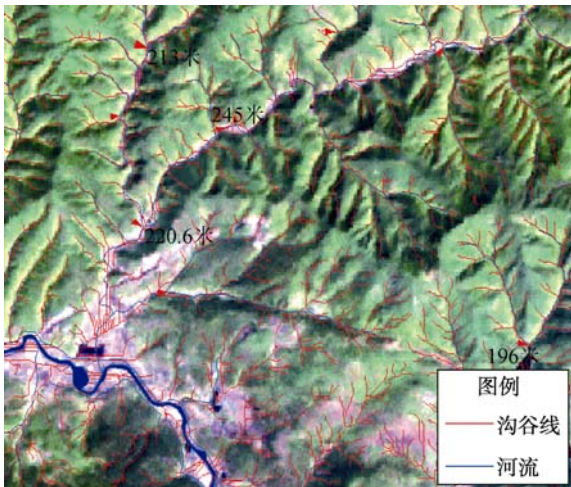


图4 沟谷线、水系和卫星图像的叠加显示

3.4 控制点采集与纠正处理

用 AML 编写控制点采集程序, 实现控制点的增加、删除、存盘和退出等, 进行控制点的交互式批量采集。在安宁 1000 km² 多的区域, 建立的 FGCP 文件中的控制点达到 1175 个。采集控制点时, 选择卫星图像上可视效果好的地性线的交叉点、拐点为控制点, 并保障任何小的局部区域应有控制点分布。安宁市地形较为破碎、起伏大, 使用沟谷线可以得到密集的控制点, 所以, 实验中的控制点以沟谷线为主。

3.5 基于地性线的精纠正与误差估计

在 Workstation 环境下进行纠正处理, 得到了配准效果完美的图像, 卫星图像所表达的可视地形特征与绝大多数沟谷线实现了准确配准。

建立度量间隔为 0.02° 的经纬网, 对网格进行编码, 随机抽样后得到 20 个点的小样本, 见图 5。对经纬网地图进行投影, 以沟谷线作为真值, 使用交互式方法测量选中为样本点的网格顶点上的误差, 得到样本数据(表 1)。

应用公式(2)求得样本的平均误差及标准差为:
 $\Delta X=30.453$ $s=1.381$ 。

取置信度为 90%, 查自由度为 19 的 t 分布的双侧分位数表得 $t_{\alpha/2}(19)=1.729$, 利用式(3), 求得总体误差的区间估计为: (29.92, 30.99)。

试验结果表明, 平均几何误差不超过 1 个像元,

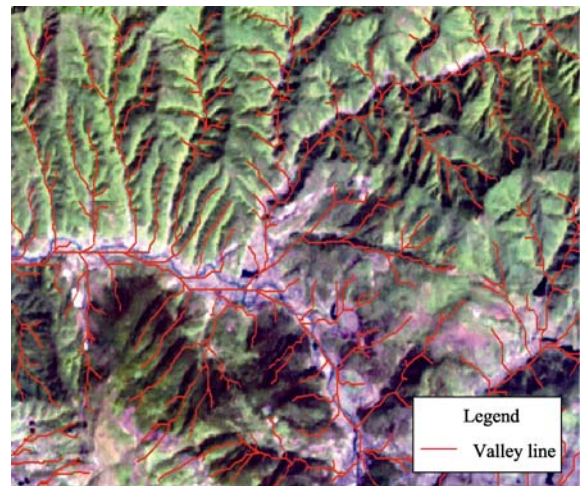


图5 控制点采集的交互界面

表1 用于误差估计的样本点

编号	误差/m
01	28.63
02	16.98
03	30.35
04	41.55
05	26.88
06	34.28
07	56.35
08	29.86
09	22.32
10	46.53
11	34.63
12	12.87
13	22.23
14	9.11
15	35.30
16	24.16
17	34.71
18	24.68
19	42.40
20	35.24

即 30m。以 90%把握可断定, 其纠正的误差在 29.92—30.99m 之间。

4 结论与讨论

通过以上研究, 可以得出如下结论:

(1) 提出了一种基于地性线控制纠正山地区域卫星遥感图像的理论和方法, 该方法利用基于 DEM 的地性线精确表达地形的起伏特点, 并以其为基准对山地区域上的卫星遥感图像的随机几何变形进行精纠正。

(2) 基于 DEM 的地性线代替传统的控制纠正地图层, 提高了控制线的数量级别, 解决了控制点难找、控制点不足的问题。

(3) 该方法适合有地形起伏区域的山地区域卫星图像的几何精纠正。

(4) 实验结果表明, 精纠正图像的几何误差不超过 1 个像元。

对于 10 m 级以上分辨率的卫星遥感图像, 由于小的道路、水系等地性线不可视, 几何精纠正中出现了控制点难找、控制点不足的问题; 特别是多山地区, 由于投影差的影响, 控制点太少, 某些局部区域的纠正效果不好。具有地形起伏的地方有沟谷线、山脊线, 利用 DEM 可以将其提取出来, 用以控制纠正卫星图像, 可以解决该应用问题。

在地性线提取过程中, 阈值的选择有一定难度; 如果取值太小, 小的地形特征不能有效提取, 如果取值太大, 大的地形特征不能表达为线性数据。今后, 可以考虑探讨多分辨率数据、多阶段提取来获得不同尺度的地性线数据。

在地形变化起伏较小的地区, 人为夸大高程的比, 可使较平坦地区的地形有较大起伏, 用该方法提取地形较平坦地区的地性线的方法值得探索。

在地形的反转变换中, M 的数值可选在最高高程的 1.5—2 倍之间取值, 对分析结果没有影响, 其本质是一个简单线性变换。今后, 可以考虑使用反比例变换来反转地形, 但应用效果还需进一步探讨。

在控制点采集过程中, 由于视觉的作用, 一般来说卫星反立体影像与沟谷的特征线的对应关系容易找, 与山脊线的对应特征难找, 当然, 地表的长期侵蚀的作用, 一般山头的脊线相对平坦也是原因之一。把所有空间数据旋转 180° , 可能是采集山脊线控制点的一种方法, 但本研究未加以探索。

文中误差估计使用了数理统计中点估计和区间估计来估计精纠正的误差。利用中误差估计方法计算出来的误差为 33.25m, 为图像上一个像元左右, 与文中的误差估计近似。由于衡量本研究精纠正效

果的好坏是看纠正后的地物与地形线的距离大小, 不区分差值的正负, 所以使用文中的误差估计便可以衡量出纠正的精确度。

由于 ETM 多波段图像分辨率为 30m, 当图像放大到 1 : 2 万比例尺左右时, 马赛克效应影响了肉眼识别与选取控制点, 也影响了误差量测与评估。使用多波段数据融合、亚像元分解与图像增强, 可以大大提高卫星图像的视觉效果, 提高可视比例尺。

REFERENCES

- Chen Y L and Qin J. 2005. Geometric correction for pretreatment of landsat-7 satellite image. *Railway Investigation and Surveying*, (4): 16—18
- Deng X J and Zhu J J. 2006. The geometric rectification of QuickBird images. *Modern Surveying and Mapping*, **28**(6): 40—41
- Emery W J. 1989. AVHRR image navigation: summary & review. *Photogrammetric Engineering and Remote Sensing*, **55**(8): 1175—1183
- Huang J F, Xu H W and Wang R C. 2000. Accurate geometric correction for NOAA/AVHRR data. *Journal of Zhejiang University (Agric. & Life Sci.)*, **26**(1): 17—21
- Jiang G M, Liu R G and Niu Z. 2004. An optimal geometric correction method for MODIS 1B data collection and its software development. *Journal of Remote Sensing*, **8**(2): 158—163
- Lip Donald. 1994. A one-step algorithm for correction and calibration of AVHRR level 1B data. *Photogrammetric Engineering & Remote Sensing*, **60**(2): 165—171
- Ren L C, Zhu C G and Zheng K. 2001. SOMP geometric exact correction method of TM image. *Journal of Remote Sensing*, **5**(4): 295—299
- Wang W Y. 1999. A study of forest fire monitoring by satellite and the relative problem of information transmission. *Forest Fire Prevention*, (4): 35—36
- Zhao B Y and Jing X F. 2000. Study of geometric correction technology and methods for TM data. *Soil and Water Conservation in China*, (6): 30—32
- Zhao J A, He R Y and Zhang S G. 2007. Geometric precision correction of the ETM+ Pan imagery. *Computer Simulation*, **24**(6): 199—202

附中文参考文献

- 陈于林, 秦军. 2005. LANDSAT 7 卫星图像预处理的几何纠正. *铁道勘察*, (4): 16—18
- 邓晓嘉, 朱建军. 2006. QuickBird 遥感影像的几何校正. *现代测绘*, **28**(6): 40—41
- 黄敬峰, 许红卫, 王人潮. 2000. NOAA/AVHRR 数据的几何精纠正方法研究. *浙江大学学报 (农业与生命科学版)*, **26**(1): 17—21
- 蒋耿明, 刘荣高, 牛铮. 2004. MODIS 1B 影像几何纠正方法研究及软件实现. *遥感学报*, **8**(2): 158—163
- 任留成, 朱重光, 郑柯. 2001. TM 图像的 SOMP 几何纠正法. *遥感学报*, **5**(4): 295—299
- 王文元. 1999. 卫星林火监测及信息传输有关问题的探讨. *森林防火*, (4): 35—36
- 赵帮元, 荆小峰. 2000. TM 卫星影像几何纠正技术方法浅探. *中国水土保持*, (6): 30—32
- 赵君爱, 何瑞银, 张士国. 2007. ETM+ 全色波段影像的几何精校正. *计算机仿真*, **24**(6): 199—202